Change detection by new DSmT decision rule and ICM with constraints : Application to Argan land cover

Azeddine Elhassouny*
IRF-SIC Laboratory
Faculty of science
Agadir, Morocoo
Email: info_azeddine@yahoo.fr

Soufiane Idbraim
IRF-SIC Laboratory
Faculty of science
Agadir, Morocoo
soufianeidbraim@yahoo.fr

Driss Mammass
IRF-SIC Laboratory
Faculty of science
Agadir, Morocoo
mammass@univibnzohr.ac.ma

Danielle Ducrot
CESBIO Laboratory
Toulouse, France
danielle.ducrot@cesbio.cnes.fr

Abstract—**The objective of this work is, in the first place, the integration in a fusion process using hybrid DSmT model, both, the contextual information obtained from a supervised ICM classification with constraints and the temporal information with the use of two images taken at two different dates. Secondly, we have proposed a new decision rule based on the DSmP transformation to overcome the inherent limitations of the decision rules thus use the maximum of generalized belief functions.The approach is evaluated on two LANDSAT ETM+ images, the results are promising.**

I. INTRODUCTION

The management and the follow-up of the rural areas evolution are one of the major concerns for country planning. The satellite images offer a rapid and economic access to accurate homogeneous and updated information of studied territories. An example of application which results from this is related to the topic of the changes cartography, in this paper, we are interested to study the most subtle changes of the Argan land cover and other themes in the region of Agadir (Morocco) by contextual fusion /classification multidates based on hybrid DSmT model [1]–[3] and ICM with constraints [4], [5].

Our work environment, is the theory of Dezert-Smarandache [1]–[3] which is recent and very little implemented or used before the covered work of this paper, it was applied in multidate fusion for the short-term prediction of the winter land cover [6]–[10] and, recently, for the fusion and the multidate classification [11]–[14], although the theory of evidence, it is more exploited for fusion/classification [11], [12], [15]–[19] also, for classifier fusion [20]–[22].

Our methodology can be summarized as following, after preprocessing of the images, a supervised ICM classification with constraints [4], [5] is applied to the two images, in order to recover the probabilities matrices for an after using in a step of fusion/classification basing on the theory of plausible and paradoxical reasoning known as Dezert-Smarandache Theory (DSmT) which allows to better assign the suitable pixels to the appropriate classes and also to detect the changes.

In this paper, in *section* 2, we describe in further detail the mathematical basis of the recent theory of plausible and paradoxical reasoning (DSmT), and give a description of our decision rule. The background and the details of the ICM algorithm with constraints are presented in *section* 3. In *section* 4, we provide the results of our experimentation where the algorithm was applied to a LANDSAT ETM+ image, the classification results are discussed in the same section followed by conclusions in section 5.

II. DEZERT SMARANDACHE THEORY ($DSmT$)

A. Principles of the DSmT

The DSm theory was conceived jointly by Jean Dezert and Florentin Smarandache [1]–[3], it is a new way of representing and fusioning uncertain information. DSmT, considered as a generalization of the evidence theory of Demspter-Shafer [15], was developed to overcome the inherent limitations of DST (Dempster-Shafer Theory) [1]–[3], [6]–[9], [13], [15]. The basic idea of DSmT rests on the definition of the *hyper power set*, from which the mass functions, the combination rules and the generalized belief functions are built.

The *hyper power set* D^Θ is defined as the set of all composite propositions/subsets built from elements of Θ with $\cup$ and $\cap$ operators such as:

We define *hyper power set*, D^Θ as follow :

1) $\phi, \theta_1, \theta_2, ...\theta_n \in D^\Theta$
2) If $X, Y \in D^\Theta$, then $X \cup Y \in D^\Theta$ and $X \cap Y \in D^\Theta$.
3) No other elements belong to D^Θ, except those obtained by using rules 1) and 2) [1]–[3].

with $\Theta = \{\theta_1, \theta_2, ...\theta n\}, \phi$ is empty set.

We define a map as follows:

$$m_s(.) : D^\Theta \to [0, 1] \qquad (1)$$

associated to a given body of evidence s as

$$m_s(\phi) = 0 \qquad (2)$$

and

$$\sum_{X \in D^\Theta} m_s(X) = 1 \qquad (3)$$

with $m_s(X)$ is called the basic belief assignment/mass (bba) of X made by the source s.

The DSmT contains two models : the free model and the hybrid model [**?**], [1], [2], [7], [9], [11], the first presents limits concerning the size of the *hyper power set* D^{Θ}, whereas the second has the advantage of minimizing this size, for this reason, it will be used in the continuation of our study.

B. Combination rules

The masses from the sources must be combined using a combination rule to have a new masses distribution for the elements of the *hyper power set* in order to promote an item compared to others.

Within the framework of DSmT, there are several rules combination [1]–[3], [13], in our application, we have applied and implemented the majority of these rules in order to choose those which allow us to have good performances such as the PCR5(conflicts proportionally with respect).

C. Generalized belief functions

From the function of basic mass, the generalized belief functions are defined , which model the imprecision and the uncertainty according to the hypothesis considered by a given source.

The generalized belief functions used in this study namely the Credibility (Cr), Plausibility (Pl) and DSmP Transformation are defined for D^{Θ} in $[0,1]$ and are given respectively by: Belief, plausibility and DSmP of an element $X \in D^{\Theta}$:

$$Bel(X) = \sum_{\substack{v \subseteq X \\ v \in D^{\Theta}}} m(v) \qquad (4)$$

$$Pl(X) = \sum_{\substack{v \cap X \neq \phi \\ v \in D^{\Theta}}} m(v) \qquad (5)$$

$$\begin{cases} DSmP_{\epsilon}(\phi) = 0 \\ \forall X \in G^{\Theta}\{\phi\}, DSmP_{\epsilon}(X) = \\ \\ \sum \dfrac{\sum_{\substack{Z \subseteq X \cap Y \\ C(Z)=1}} m(Z)+\epsilon \cdot C(X \cap Y)}{\sum_{\substack{Z \subseteq Y \\ C(Z)=1}} m(Z)+\epsilon \cdot C(Y)} m(Y) \end{cases} \qquad (6)$$

where $\epsilon \geq 0$ is an adjustment parameter and D^{Θ} possibly reduced by the introduction of the integrity constraints of the hybrid DSmT model. $C(X \cap Y)$ and $C(Y)$ respectively indicate the cardinalities of the $Y \cap X$ and Y.

D. Proposed decision rule

The decisions after combinations could be taken from generalized belief functions, to decide the belonging of a pixel to a given class, two cases are distinguished:

- The pixel belonging to a simple class (used to improve a classification): in this case we use one of the following decision criteria: maximum of bba, maximum of the Credibility (Cr) (with or without rejection), maximum of the Plausibility (Pl), Appriou criterium, $(DSmP$ criterium $\cdots$ etc) [6], [7], [11], [13] .
- The pixel belonging to a composed class(e.g. in the case of change detection), in this case we cannot use the functions quoted previously because they are increasing functions and unsuited to the decision for the elements of union and of intersection.

In an original step, we have proposed a new decision rule based on DSmP transformation and confidence interval to take in account the composed classes. In this decision rule we exploited the confidence interval $[Bel(X)), Pl(X)]$ by the definition of a new measurement which we have named : Global uncertainty $IncG$ which is the sum of the uncertainties (Inc) of the *hyper power set* elements:

$$\forall X \in D^{\Theta} \; Inc(X) = Pl(X) - Bel(X) \qquad (7)$$

This new decision rule described in Algorithm 1 is applied as follows:

For a given pixel x, we compare the Global uncertainty $IncG$ of this pixel with a threshold (chosen experimentally). If it is lower than this threshold, the pixel is affected to the simple class which maximizes the DSmP transformation of all the simple classes, if not, it is affected to the composed class which maximizes the mass (gbba) of all the composed classes.

Algorithm 1 The proposed decision rule

1: $IncG = \sum_{X \in D^{\Theta}} (Pl(x) - Bel(x))$
2: **if** $(IncG \leq threshold)$ **then**
3:     **if** $DSmP[x](\theta_i) = max\{DSmP[x](\theta_i)$ $with \; 1 \leq i \leq n$ **then**
4:         $x \in \theta_i$
5:     **end if**
6: **else**
7:     **if** $m[x](\cap\theta_i) = max\{[x](\cap\theta_i)$ $with \; 1 \leq i \leq |D^{\Theta}| - (n+1)$ **then**
8:         $x \in \cap\theta_i$
9:     **end if**
10: **end if**

III. ICM CLASSIFICATION WITH CONSTRAINTS

The information contained in a satellite image is usually in the form of homogeneous objects. Indeed, an image of rural areas often consists of large homogeneous parcels, and therefore, an acceptable classified image must respect this property. Thus, the use of Markov Random Fields (MRF) takes in account this property of the neighborhood influence of a pixel on it. and therefore insists on coherence between the class of a pixel and that of its neighbors. It is a powerful mathematical tool for regularizing the classification of the satellite images.

Moreover, the Markovien formalism constitutes a gateway to introduce a several constraints (spatial context, map of

contours, temporal context, etc), for this reason, we have used the suggested method by [4], [5] as a method of classification in order to generate the probabilities for DSmT. This technique of classification provides, in addition to the constraint of regularization, a new constraint of segmentation so to refine the classification. these contextual constraints are controlled by a parameter of temperature in an iterative algorithm of optimization ICM (Iterated Conditional Mode).
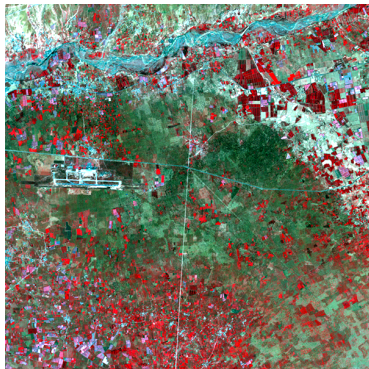
IV. RESULT AND DISCUSSION
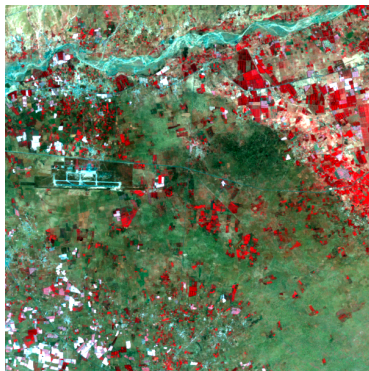
A. Study area and used data

The study area is located in the region of Souss, it is in southern Morocco. Geologically, it is the alluvial basin of the Oued Souss, separated from the Sahara by the Anti-Atlas mountains. The natural vegetation in the Souss is savanna dominated by the Argan (Argania spinosa), a local endemic tree found nowhere else, part of the area is now a UNESCO Biosphere reserve to protect this unique habitat.

The satellite images used in this study were taken respectively, in 19 March 2002 and 12 April 2005 by the Landsat ETM+, and are defined by the coordinates (Path 203, Row 39).

Figure 1 shows RGB composite of the two used images.

(a) Landsat ETM+ 2002

(b) Landsat ETM+ 2005

Fig. 1: RGB composite of the Landsat ETM+ images 2002 and 2005 (Agadir, Morocoo)

B. Trainings samples

The samples are created automatically by using the $ENVI4.0$ software. We have identified 5 topics of land occupation: $Argan$ (A), $Built/Oued$ (BO), $Vegetation$ (V), $Greenhouses$ (Gh) and $Bareground$ (Bg) while basing on images already classified and on the ground truths, the figure 2 represents their spectral responses..
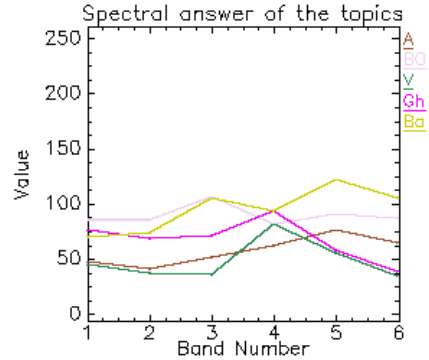

Fig. 2: Spectral response of the topics

C. ICM classification with constraints

After preprocessing of the two images and establishment of the samples, a supervised contextual ICM classification with constraints [4], [5] is applied to the two images to have the probabilities of pixels belonging to classes. The classified image of 2002 is presented in figure 3.
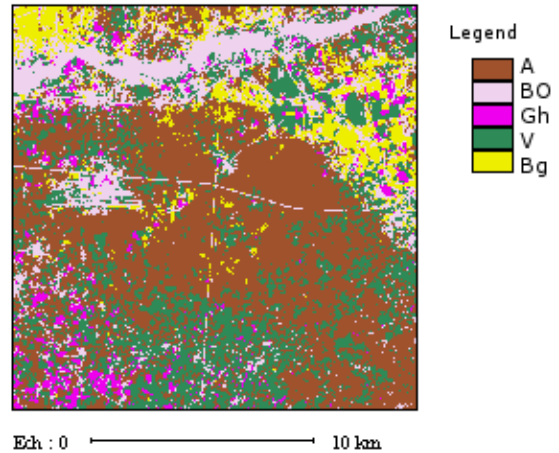

Fig. 3: Supervised ICM classification with constraints of the 2002 image (Agadir, Morocco)

D. Multidates and multi-source fusion by the hybrid DSmT model

Our fusion process is composed of the following steps, first the definition of the framework Θ, then, the estimation of the mass functions of each focal element by the model of Appriou, finally, the application of the hybrid DSmT model.

1) Hyper power set : Taking in consideration the prior knowledge of the study area, we have identified 5 classes constituting the framework Θ (*section* 4.4), which are: $Argan$ (A), $Built/Oued$ (BO), $Vegetation$ (V), $Greenhouses$ (Gh) and $Bareground$ (Bg).

So, Θ is defined as follows: $\Theta = \{A, BO, Gh, V, Bg\}$

Exploiting information of the study area and also those obtained by ICM classifications with constraints, some elements of the *hyper power set* D^Θ seem not being adjacents and exclusives. To realize a better adapted study to the real situations, some exclusivity constraints will be taken (hybrid DSmT model), for example $A \cap Gh = \phi$, which reduces the number of focal elements of the D^Θ.

2) Choice of threshold: The decision is made for the simple classes and the classes of intersection by using our rule decision defined previously (*section* 2.5), the threshold should be determined in advance by experimentation and analysis of total uncertainty distribution after standardization, wich is presented in figure 4.
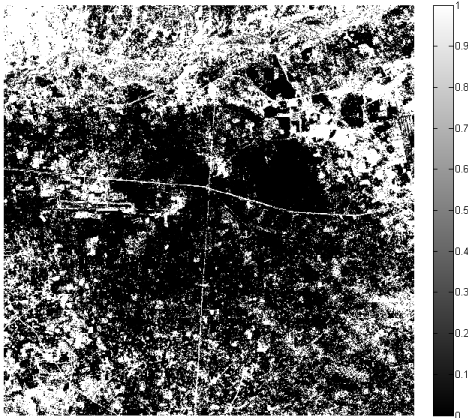

Fig. 4: The standardized global uncertainty distribution of the fusion map

We have tested our decision rule with various values of threshold, the following table I presents the occupancy rates of the simple classes (stable zones) and composed classes (change zones) according to the threshold.

TABLE I: Occupancy rates of the simple classes and the composed classes according to the value of the threshold

value of the threshold	(%)of stable zones	(%)of change zones
1.0e-26	0%	100%
1.0e-019	9.64%	90.36%
1.0e-016	32.12%	67.88%
1.0e-014	54.408%	45.592%
1.0e-012	76.86%	23.32%
1.0e-08	99.99	%0.01%

The choice of threshold depends to the good results of detection with the use of the changed/ unchanged samples between the two dates (2002 and 2005), for this we have taken a suitable threshold that equal to $1.0e^{-14}$.

The results obtained with the various values of the threshold are as follows: a map contains 100% of the composed classes

for the threshold of $1.0e-26$, 0.01% for the threshold of $1.0e-8$ and 45.592% for the threshold of $1.0e-14$. The first result does not match with the ground truths because several areas of the region are unchanged during the considered period. The second result is far from the dynamic reality of the region that has known a great change. The last result is coherent and appears to be close to reality basing on the test samples of the stable zones and the zones of changes between the two images, while for thresholds which exceed the surrounding of $(1.0e-14)$ there is a degradation of the change detection

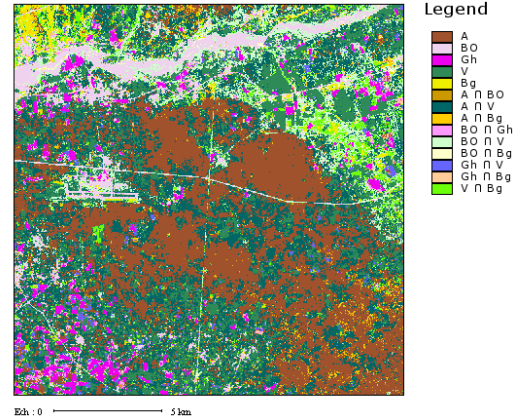*3) Validation of the results:* The fusion map obtained with an adequate threshold =(1.0e-14) is presented in figure 5.

Fig. 5: Fusion map obtained with threshold of (1.0e-14)

From the fusion map, obtained with an adequate threshold we obtain the table II presenting the occupancy rate of the classes.

TABLE II: Occupancy rate of the classes

Classes	(%)
A	29.04%
BO	4.869%
Gh	3.18%
V	15.92%
Bg	1.399%
$A \cap BO$	0.649%
$A \cap V$	26.40%
$A \cap Bg$	1.87%
$BO \cap Gh$	1.549%
$BO \cap V$	7.25%
$BO \cap Bg$	1.08%
$Gh \cap V$	1.98%
$Gh \cap Bg$	0.5%
$V \cap Bg$	3.30'%

The table II illustrates the occupancy rates of the stable zones (simple classes) which reaches the rate of 54.408% and that of the zones of change (composed classes) which reaches 45.592%. From the table II, we note that the Argan class (A) and Vegetation class (V) have known a great change compared to the other classes, Indeed, we found for the composed class $(A \cap V)$ a rate of change of 26.40%.

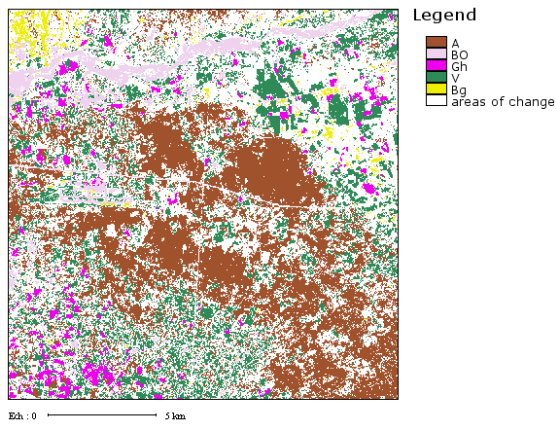The figure 6 presents the stable zones map obtained from the fusion map.

Fig. 6: Stable zones map

From the stable zones map, we note that the zone of Oued Souss (BO), the zone of the urban areas along the road Agadir-Taroudant (BO), the international airport of Almassira (BO), the parcels of the Ouled teima region (V), the greenhouses (Gh) of the Biogra region and also some surface of argan (A) are all well detected as stable zones and are assigned to simple classes. This attribution is well justified because some zones are built and are unchangeable by nature. For the change zones, figure 7 illustrate those zones obtained from the fusion map after post-processing.
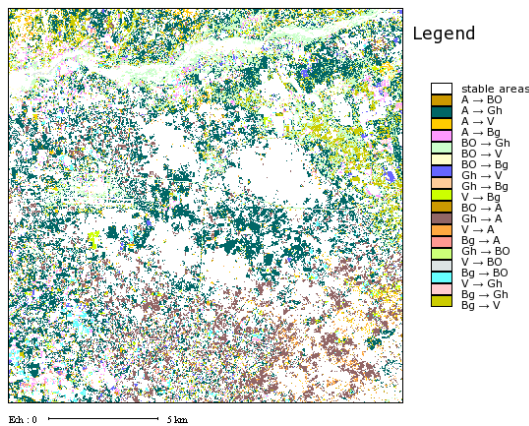

Fig. 7: Post-processed map of change zones obtained from fusion map

In the post-processed fusion map, areas that have known major changes are the Argan class wich becomes bare ground or vegetation, which is well explained because of the defor-estation. As result we found a rate of 18.95 of the Argan class changed to vegetation in 2005.

a) validation per spectral signature of the results: To evaluate our proposed method, we have chosen to use spectral signatures of classes (themes) for the two images. For pixels of change areas , we have a variation in the spectral signature of the image pixels between 2002 and 2005. Conversely, the pixels of the stable areas have shown a stability of spectral signature between the two dates.

For this spectral evaluation, we have used the zoom window of the $ENVI4.0$ software for the images ETM+ 2002, ETM+ 2005 and the fusion map to link them for locating the change zones in the fusion map (figure **??**), Then we have compared the spectral signatures of the same area for the two images by taking in account the distributions of spectral signatures of different themes.

The following figures 8 present an example of validation of the change results.

(a) ETM+ 2002 (b) ETM+ 2005 (c) Fusion map

(d) Spectral signature of V (ETM+ 2002) (e) Spectral signature of A (ETM+ 2005)
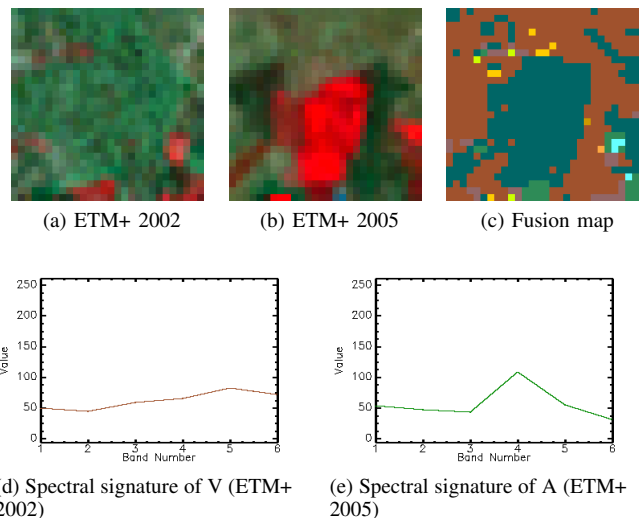
Fig. 8: Spectral signature of the Argan class (A)(ETM+ 2002) and of the Vegetation class (V) (ETM+ 2005)

From the figure 8, we note that the extract area has known a change of Argan theme (Class A) to vegetation theme (class V), what is shown by the change of the pixels spectral signature of the extract area which had in 2002 a spectral signature of the Argan (Class A), and became in 2005 that of the vegetation (Class V).

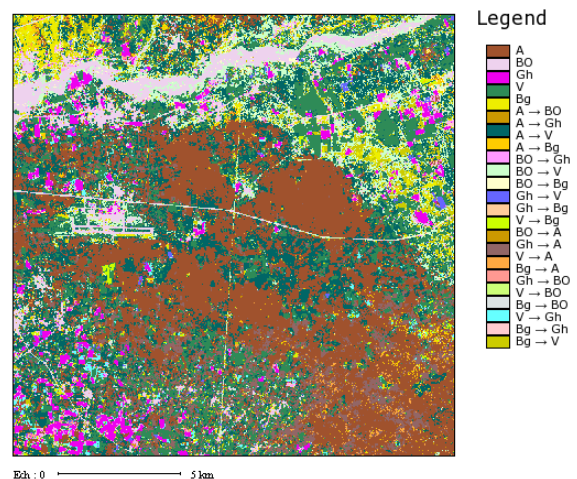The figure 9 shows the post-processed map of the fusion.

Fig. 9: Post-processed fusion map

The table III illustrates the detection of the change by fusion

TABLE III: Rate of change obtained by fusion between LANDSAT ETM+ 2002 and ETM+ 2005

Classe	Number fo pixels	Occupancy rate(%)
A	104,542	29.0394
BO	17,538	4.8717
Gh	11,458	3.1828
V	57,320	15.9222
Bg	5,048	1.4022
$A \rightarrow BO$	797	0.2214
$A \rightarrow V$	68,202	18.9450
$A \rightarrow Bg$	4,295	1.1931
$BO \rightarrow Gh$	4,650	1.2917
$BO \rightarrow V$	25,587	7.1075
$BO \rightarrow Bg$	3,227	0.8964
$Gh \rightarrow V$	3,112	0.8644
$Gh \rightarrow Bg$	471	0.1308
$V \rightarrow Bg$	2,662	0.7394
$V \rightarrow A$	26,889	7.4692
$Bg \rightarrow A$	2,439	0.6775
$Gh \rightarrow BO$	915	0.2542
$V \rightarrow BO$	502	0.1394
$Bg \rightarrow BO$	647	0.1797
$V \rightarrow Gh$	4,005	1.1125
$Bg \rightarrow Gh$	1,324	0.3678
$Bg \rightarrow V$	12,831	3.5642

with :Argan(A), Built/Oued (BO), Greenhouses (Gh), Vegetation (V), Bare ground (Bg).

V. Conclusion

In this paper we have proposed a new method for land cover changes detection. In first, we have included the spatial information in the process of fusion/classification by using a hybrid DSmT model with the introduction of contextual information using ICM classification with constraints, the use jointly of DSmT and ICM improves performance of the changes detection in terms of accuracy and exactitude. Secondly, we have proposed a new decision rule that has shown its performance and allowed us to overcome the limitations of rules decision based on the maximum generalized belief functions which are increasing and unsuited to the decision of the union and the intersection of elements.

The application of this method for the catography of the land cover changes is promising, however, the determination of the adequate decision rule (currently we work on a dynamic fusion method) and the addition of a temporal constraint to allow the processing of different dates are still significant issues for further investigation.

References

[1] F. Smarandache, J. Dezert (Editors), Advances and Applications of DSmT for Information Fusion (Collected works), vol. 1, American Research Press, Rehoboth, U.S.A., 2004.

[2] F. Smarandache, J. Dezert, Advances and Applications of DSmT for Information Fusion (Collected works), vol. 2, American Research Press, Rehoboth, U.S.A., 2006.

[3] F. Smarandache, J. Dezert, Applications and Advances of DSmT for Information Fusion (Collected works), Vol. 3, American Research Press, Rehoboth, ARP 2009.

[4] S. Idbraim, D. Ducrot, D. Mammass, D. Aboutajdine, An unsupervised classification using a novel ICM method with constraints for land cover mapping from remote sensing imagery, International Review on Computers and Software (I.RE.CO.S.), Vol. 4, no. 2, 2009.

[5] D. Ducrot, Méthodes d'analyse et d'interprétation d'images de télédétection multi-sources Extraction de caractéristiques du paysage, habilitation thesis, France, 1er décembre 2005.

[6] G. Mercier, Outils pour la télédétection opérationnelle, habilitation thesis, Rennes I university, France, 2 March 2007.

[7] S. Corgne, L. Hubert-Moy, J. Dezert, G. Mercier, Land cover change prediction with a new theory of plausible and paradoxical reasoning, ISIF2003, Colorado, USA, March 2003.

[8] F. Smarandache, J. Dezert, An Introduction to the DSm Theory for the Combination of Paradoxical, Uncertain and Imprecise Sources of Information, Information&Security International Journal, 1st August 2006.

[9] B. Moraa, R. A. Fourniera, S. Foucherb, Application of evidential reasoning to improve the mapping of regenerating foreststands, International Journal of Applied Earth Observation and Geoinformation, 2010.

[10] R. M. Basse, Université de Nice, La prise en compte de l'incertitude dans une démarche de modélisation prédictive, MoDyS, Lyon, France, 8 and 9 Novembre 2006.

[11] A. Bouakache, A. Belhadj-Aissa, Satellite image fusion using Dezert-Smarandache theory, DSmT-book3, Master Project Graduation, University Houari Boumediene, 2009.

[12] R. Khedam, A. Bouakache, G. Mercier, A. Belhadj-Aissa, Fusion multidate à l'aide de la théorie de Dempster-Shafer pour la détection et la cartographie des changements : application aux milieux urbain et périurbain de la région d'alger, Télédétection, Vol. 6, no. 4, pp. 359 404, 2006.

[13] P. Djiknavorian, Fusion d'informations dans un cadre de raisonnement de Dezert-Smarandache appliquéE sur des rapports de capteurs ESM sous le STANAG 1241, Memory to obtain the degree (M.Se.), Laval University, Quebec, 2008.

[14] J. Anne-Laure, A. Martin, P. Maupin, Gestion de l'information paradoxale contrainte par des requêtes pour la classification de cibles dans un réseau de capteurs multi-modalités, SCIGRAD08, Brest, France, 24-25 novembre 2008.

[15] S. Foucher, M. Germain, J. M. Boucher, G. B. Bénié, Multisource Classification Using ICM and Dempster-Shafer Theory, IEEE Transaction on Instrumentation and Measurement, Vol. 51, no. 2, APRIL 2002.

[16] I. Bloch, Fusion d'informations en image et vision, ENST - CNRS UMR 5141 LTCI, Paris - France.

[17] Y. Lemeret, E. Lefevre, D. Jolly , Fusion de données provenant d'un laser et d'un radar en utilisant la théorie de Dempster-Shafer, MAJEC-STIC'04, France, 2004.

[18] A. Fiche, A. Martin, Bayesian approach and continuous belief functions for classification, LFA, Annecy, France, 5-6 November 2009.

[19] M. Germain, J. M. Boucher, G. B. Bénié, E. Beaudry, Fusion évidentielle multi source basée sur une nouvelle approche statistique floue, ISIVC04, Brest, France, 2004.

[20] A. Martin, Fusion de classifieurs pour la classification d'images sonar, RNTI-E-5, pp 259 268, novembre 2005.

[21] S. Chitoub, Combinaison de classifieurs : une approche pour l'amélioration de la classification d'images multisources multidates de télédétection, Télédétection, vol. 4, no. 3, pp. 289 301, 2004.

[22] R. Sitraka, R. Solofoarisoa, R. Solofo, Combinaison de classificateurs selon la théorie de Dempster -Shafer pour la classification d'images satellitaires, Mada-Go13 (ISSN 2074 4587), Mai 2009.